The Microscopic Switching Mechanism of a [2]Catenane

M. Ceccarelli,*,† F. Mercuri,‡ D. Passerone,§,⊥ and M. Parrinello*,||

Department of Physics and INFM/SLACS, University of Cagliari, 09042 Monserrato, Italy, ISTM-CNR, c/o Department of Chemistry, University of Perugia, 06123 Perugia, Italy, Computational Laboratory (CoLab), ETH Zurich, Switzerland, and Computational Science, Department of Chemistry and Applied Biosciences, ETH Zurich, Switzerland

Received: March 30, 2005; In Final Form: June 22, 2005

We apply numerical simulations at an all-atom level to investigate the switching mechanism of a [2]catenane, a prototype of a molecular machine. This system is able to switch reversibly between two different stable states, upon external stimuli, with a time scale ranging from microseconds up to milliseconds, well over the typical domain of molecular dynamics (MD) computer simulations. However, combining a strategy recently developed for investigating rare events with ordinary MD, we are able to unravel the microscopic mechanism of the conformational rearrangements involved in the switching process, including dynamical effects. Along the path that connects the product and reactant state, we find several intermediate states characterized by $\pi-\pi$ stacking interactions and hydrogen bonds. Moreover, counterions interact strongly with the system in a correlated way, in agreement with recent static calculations performed on [2]rotaxanes.

1. Introduction

Molecular machines, obtained by the self-organization of simple molecular units,[2−5] are usually controlled by conformational changes related to a specific movement (switching, shuttling, etc.) performed by one part of the molecule with respect to the others. Such changes, essentially reorganizations of supramolecular interactions, are generally induced by applied external stimuli like light (photons) or chemical energy (oxido-reduction reactions). The time scale of such processes, ranging from microseconds to milliseconds, lies beyond typical time scales of standard MD simulations. Indeed, the large number of degrees of freedom involved and the presence of a rough potential energy surface characterized by different minima separated by large energy barriers make MD simulations rather problematic: systems initialized in one minimum have a negligible probability of sampling other relevant parts of phase space unless some drastic approximation is made. This is a serious shortcoming since numerical simulations together with experiments are essential for a full understanding of microscopic processes in complex systems.

To solve this problem, many different methods have been advocated. However, the majority of these approaches are focused on recovering the main features of the energy or free energy surfaces.[6,7] Notable exceptions are transition path sampling (TPS)[8,9] and action-derived dynamics (ADD),[10,11] which aim at reconstructing the real dynamics. In TPS, the dynamical trajectories that connect two basins are generated and sampled via a procedure that requires an initial trajectory, whereas in ADD, they are obtained through an appropriate application of the well-known variational principles of classical mechanics. In principle, ADD appears to be a more straightforward procedure since one needs only the initial (A) and final (B) positions of the system, and by making the appropriate action stationary, the dynamical trajectory connecting A to B can be determined. In fact, ADD is a way of solving Newton's equations by using different boundary conditions, namely, the initial and final positions, rather than the initial position and velocity, as is usually done. However, finding the stationary point of the action is not easy since trajectories usually correspond to a saddle point of the action and are difficult to determine with accuracy. It is, therefore, important to assess how far the ADD trajectories depart from the Newtonian ones and to what extent they are representative of the real dynamics. In this paper, we show how ADD and standard MD simulations can be combined to complement each other to obtain the essential dynamical effects occurring within a rare event. We apply this strategy to the investigation of the switching mechanism of a [2]catenane, a prototype of a molecular machine.

The interest in [2]catenanes arises from the remarkable body of recent studies, mainly carried out in the groups of Stoddart and co-workers,[12] demonstrating the effective functionality of this molecule as a fully reversible, bistable molecular switch. Furthermore, molecular switches (rotaxanes and [2]catenanes) were recently used as basic components in the realization of molecular engines, such as a molecular elevator[13] and a reversible molecular motor.[14] However, despite the large amount of experimental work on molecular-level devices and machines, many microscopic aspects of their operating mechanism remain, in most cases, unclear. In this first application, we apply MD simulations at an all-atom level to investigate the switching mechanism reported in Figure 1, without including the solvent. Nevertheless, our conclusions provide the stepping stone for future investigations on catenanes and rotaxanes in a more complex environment, such as in solution or in solid-state devices.[1,2] At the same time, our results indicate that ADD trajectories provide realistic insights into the dynamics and can be used to extract reaction mechanisms and reaction coordinates.

* Author to whom correspondence should be addressed. E-mail: matteo.ceccarelli@dsf.unica.it (M.C.); parrinello@phys.chem.ethz.ch (M.P.).
† University of Cagliari.
‡ University of Perugia.
§ Computation Laboratory (CoLab), ETH Zurich.
⊥ Present address: Institute of Organic Chemistry, University of Zurich, Winterthurerstrasse 190, 8057 Zurich, Switzerland.
|| Department of Chemistry and Applied Biosciences, ETH Zurich.

10.1021/jp051609v CCC: $30.25
Published on Web 07/27/2005

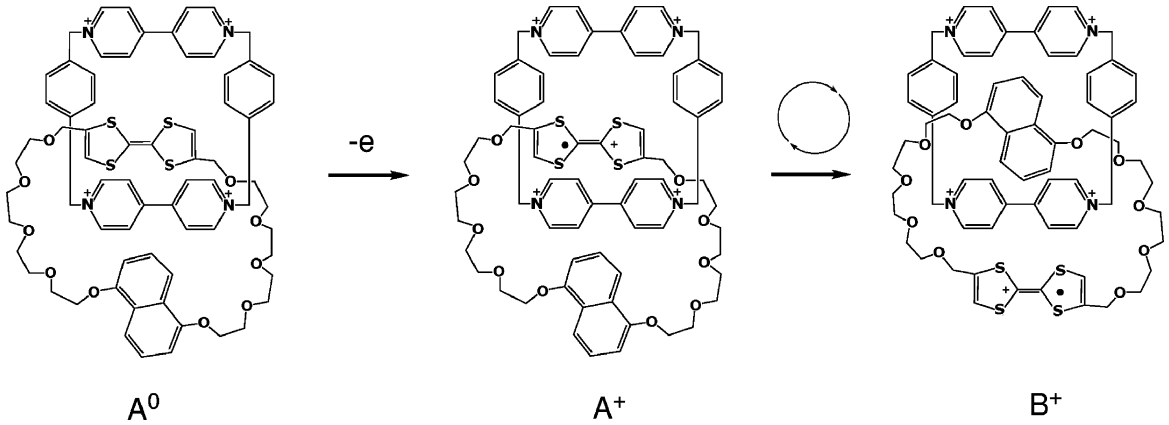

Figure 1. Scheme of our [2]catenane and its switching process.

These latter could be used, at a later stage, for reconstructing the free energy surface.[7,15]

The paper is organized as follows: Section 2 is devoted to the description of the computational strategy and 3 to the model system; in Section 4, the results obtained for the isomerization of the [2]catenane are discussed; finally, Section 5 is devoted to concluding remarks.

2. Computational Strategy

Computational studies of rare transitions between stable states, like the "switching" process studied in this paper, can profit greatly from theoretical methods in which information about the initial and final states is given. A well-known principle of classical mechanics states that the Hamilton action

$$S = \int_0^\tau L(q, \dot{q}, t)\, \mathrm{d}t \qquad (1)$$

where $L = T - V$ is the Lagrangian, is stationary relative to the variation in the $q(t)$, which obeys the boundary conditions $q(0) = q_0$ and $q(\tau) = q_1$. This, in principle, provides a means to calculate the trajectory that starts at time $t = 0$ at q_0 and ends at $t = \tau$ at q_1. Unfortunately, the Hamilton principle does not imply that the stationary point is a minimum or a maximum. In fact, it can proved to be a minimum only for very short time τ (in the present case, less than 10 fs), and in general, it is a saddle point. To remedy this situation and facilitate the search for the stationary point of S, a modified action is introduced:[10]

$$S_\Theta = \gamma \int_0^\tau L(q, \dot{q}, t)\, \mathrm{d}t + \mu \int_0^\tau (T + V - E)^2\, \mathrm{d}t \qquad (2)$$

where μ is a positive parameter for ensuring energy conservation, γ is a prefactor that can be ± 1, and E is the total energy of the system. As can be seen from eq 2, the functional is composed of two parts: the first is Hamilton's action; the second term, which enforces energy conservation, improves convergence since it can make a number of eigenvalues of the Hessian positive. The parameter μ tunes the relative weight of these two terms. In previous papers,[10,11] we tested various combinations of parameters γ and μ. For a one-dimensional system, we showed that, above a certain stability threshold, the value of μ is not critical for the quality of the path. Concerning γ, we empirically found, as a general rule of thumb, that a negative value of γ leads to a higher quality path.

This approach is affected by two problems: first of all, the second term has a lower dimensionality with respect to the first one. With this, we mean that, at a stationary point of S_Θ, its Hessian can be analyzed. The second term has strictly positive and null eigenvalues. The number of strictly positive eigenvalues, for a multidimensional system and for physically meaningful (i.e., not too large) time steps, is usually smaller than the number of negative eigenvalues of the first term. Therefore, any minimizer will most likely end up in a very "flat" zone of the trajectory space without reaching a true minimum. Therefore, there is no a priori guarantee that the trajectory obtained will be close to a Newtonian trajectory. Nevertheless, since the paths obtained with this functional are energy conserving, they can be used as starting points for another class of algorithms aimed at obtaining the stationary point of the original Hamilton action. Moreover, as we will show in this paper, the trajectories found after minimization of S_Θ and subsequent local refining can, in some sense, be representative of the realistic transition mechanism. In the past, we have applied the modified action functional to chemical reactions[16] and other simple systems. Using the conjugate residual method[11] and other algorithms capable of finding nonpositive definite stationary points, it is possible to construct a strategy for reaching a satisfactory approximation to a dynamical trajectory using the solution to the minimization of S_Θ as a starting point.

Since it is difficult to optimize very long trajectories, most ADD trajectories are rather short and tend to skip many details on the potential energy surface. Therefore, we used the description of the reactive path provided by the ADD scheme as a starting point to obtain different dynamical trajectories by a procedure that is inspired by TPS.[8] Once the region of the transition state is located along the ADD trajectory, from a number of configurations thus generated, several short trajectories are started with a set of random velocities extracted from a Boltzmann distribution. The trajectories are also propagated backward in time by inverting the initial velocities. The first goal of such a procedure consists of locating energy minima and transition states along the very short ADD reactive path. Among all trajectories originated in the described way, a successful one will be a trajectory connecting two different basins of attraction. To identify such paths, an order parameter distinguishing the different basins of attraction is defined. The successful trajectories are further prolongated back and forth for several nanoseconds. It must be stressed that this procedure differs from TPS, lacking the relaxation in the path space. Indeed, the latter is implicitly done in the ADD step. Moreover, the system considered, two interlocked rings, is constrained to rotation of one ring with respect to the other, with small space for different reactive channels in the switching mechanism. The focus of this paper is to analyze qualitatively and quantitatively the main features of the switching mechanism in a real dynamical transition.

3. Model System

Although a large part of the experimental research is concerned with the behavior of [2]catenanes in solution, where the switching mechanism has been mostly investigated,[17] potential practical applications require a coupling within a solid-state matrix,[18] as is done in ref 2. Our [2]catenane is constituted from a cyclobis(paraquat-*p*-phenylene) (CBPQ) ring interlocked with a crown ether bearing a tetrathiofulvalene (TTF) and a 1,5-dioxynaphthalene (DNP) aromatic unit located on opposite sides of the crown ether chain. In an isolated $\{[2]\text{catenane}\}^{4+}$ cation, the four positive charges are localized on the cyclophane ring (see Figure 1). This configuration can be referred to as A^0 and corresponds, as a result of strong $\pi-\pi$ stacking interactions, to the stable configuration for the [2]catenane in its nonoxidized state.[17] Upon oxidation, a further positive charge is localized on the TTF unit, yielding the [2]catenane cation with five positive charges A^+, see Figure 1. The A^+ state can be considered a metastable configuration since the repulsive interaction between the charged TTF unit and the cyclophane ring induces the circumrotational motion of one ring through the cavity of the other, leading to the co-conformer B^+, the latter being a stable configuration for the molecule in its charged state, see Figure 1. The process is fully reversible, in the sense that the reduction of B^+ induces another circumrotational motion, leading back to A^0. As suggested by Stoddart et al.,[2] a similar mechanism should occur when [2]catenanes are inserted in a solid-state device. We focused our analysis on the first part of the reversible switching mechanism, that is, the rearrangement process from one co-conformer to the other upon oxidation.

Parametrization. As a result of the long time scale of the processes under study and the size of the system (192 atoms), a fully ab initio description is not feasible. However, since such processes are mainly ruled by nonbonded forces, we find the use of classical MD with an empirical force field appropriate. Hence, MD calculations were performed by applying the AMBER[19] force field as implemented in the ORAC[20] program package. Given the relevance of electrostatic effects in determining the co-conformational rearrangement, attention was paid to the determination of the charges, which we calculate using the RESP procedure fitted from the HF/6-31G** electronic density. This computational setup provided good results when applied to similar systems.[21] Force-field parameters were tested against the X-ray crystal structure of the [2]catenane[22] by performing MD simulations on a model made up of 12 unit cells ($2 \times 3 \times 2$) in *Cc* symmetry, each containing 4 [2]catenane units, 16 PF_6^- counterions, and 24 acetonitrile molecules. We performed constant pressure MD simulations using the Parrinello−Rahman scheme[23] at room temperature for 300 ps. The shape of the crystal cell is well-reproduced apart from a small homogeneous volume dilatation (7%). The X_{RMS} deviation per atom of the whole cell (cell-fit X_{RMS}) is 0.74 Å for the atomic species constituting the [2]catenane units (see Table 1). Moreover, the structure of crystal-packed single [2]catenane units (molecule-fit X_{RMS}) are well reproduced: the average deviation per atom is 0.33 Å for all heavy atoms and reduces to 0.25 Å when the oxygens of the crown ether are excluded. Once the parameters of the force field have been validated for this case, we focused on the understanding of the microscopic mechanisms underlying the isomerization of the [2]catenane.

We simulate a model system constituted by an isolated [2]-catenane tetracation, in vacuum, surrounded by four PF_6^- counterions, the same used in experimental works concerning [2]catenanes as crystals,[22] in solution,[17] and in prototypes of solid-state devices.[2] Despite its simplicity, this model keeps the major features of a more complex system, allowing a description of the energetics involved in the co-conformational rearrangement process, strongly related to electrostatic effects, as will be discussed later. The strong electric field produced by a 4+ cation results in attractive interactions toward negatively charged species, and this plays a role in the switching mechanism. This system can also be viewed as a useful model for investigating the operating mechanism of the [2]catenane when inserted in a solid-state matrix, where charges also are present. Although the operating mechanism of molecular machines and devices[21] and, in particular, the circumrotation of macrocycles in catenanes[24] have already been addressed in previous theoretical investigations, we now describe the switching mechanism at a finite temperature, without any approximation on the dynamics.

TABLE 1: Volumes and Cell Parameters of the Simulated and Experimental Crystal Structures[a]

cell parameters	experiment	simulation
a (Å)	43.56	45.1 (± 0.2)
b (Å)	48.88	49.8 (± 0.1)
c (Å)	54.87	55.9 (± 0.1)
α	90.0°	90.1° (± 0.3)
β	93.9°	94.9° (± 0.3)
γ	90.0°	90.0° (± 0.2)
volume (Å^3)	116 563	125 014 (± 297)
cell-fit X_{RMS} (Å)		0.74 (± 0.04)
molecule-fit X_{RMS} (Å)		0.33 (± 0.01)

[a] The cell-fit X_{RMS} is defined as the deviation of the 48 [2]catenane units (averaged over 300 ps) with respect to the experimental crystal structure. The molecule-fit X_{RMS} is defined as the deviation of a single [2]catenane unit (averaged over 300 ps and 48 molecules) with respect to the experimental crystal structure.

The ADD approach requires as an input a representative of the initial and final states, A and B. For the initial state, we use a molecular arrangement for the nonoxidized system taken from our simulation of the crystal. The system is then equilibrated at 300 K. This gives a representative structure for the nonoxidized configuration A^0. To simulate the oxidized state, we renormalized the TTF charges so as to obtain an overall 5+ charged state. Such a procedure was validated through comparison with a full DFT calculation of the full molecule with its counterions using the CPMD code.[25] In the lack of experimental clues, the final state B was obtained by rotating the crown ether by hand until the DNP group lay inside CBPQ and, finally, relaxing this conformer at 300 K.

Order Parameters. Because of the large number of degrees of freedom, a reduced description is necessary to understand the mechanism at a microscopic level. Thus, the trajectories were analyzed in terms of a few order parameters. The first variable we considered was purely geometrical, describing the whole rotation of the crown ether with respect to the CBPQ unit (q_{ROT}). This variable is normalized so that it goes from 0.0 to 0.5 as the system goes from A to B. It does not distinguish between the rotation direction, which is not considered here because of the randomness of the motion.[14] Two more collective variables were chosen in order to account for $\pi-\pi$ interactions, namely, the coordination number between the aromatic units inserted in the polyether chain, q_{TTF} and q_{DNP}, and the CBPQ unit. Moreover, electrostatic effects were monitored by considering a parameter proportional to the number of hydrogen bonds (q_{NHB}) between the ether oxygen atoms and hydrogens of the CBPQ unit and the distance (q_{P1-4}) of each PF_6^- counterion from the center of mass of the CBPQ unit.

4. Results and Discussion

ADD Trajectory. We selected an initial trajectory taking 20 regularly spaced configurations from an artificial rotation path starting from A and ending in B. At this point, the discrete modified action functional was defined as a function of Fourier coefficients $a^{(n)}$ describing the oscillations of the path around a straight line, provided that the extremes are kept fixed:[11]

$$q(t) = q_A + \frac{(q_B - q_A)t}{\tau} + \sum_{n=1}^{P-1} a^{(n)} \sin\frac{n\pi t}{\tau} \qquad (3)$$

The total time for the reactive trajectory was fixed to $\tau = 3$ ps, and the total energy was set accordingly. In the definition of S_Θ, see eq 2, we use $\gamma = -1$ and μ was changed from 10^6 to 10^5 as the minimization proceeded.[10] The choice $\gamma = -1$ leads to a more realistic path, as we could verify a posteriori using different quality factors.

We used an MD-based simulated annealing (SA) procedure to minimize S_Θ with respect to the Fourier coefficients $a^{(n)}$ of eq 3. Whereas the SA scheme is more expensive from a computational point of view compared to the conjugate gradient algorithm that we used in the original implementation, we found its use necessary when dealing with what turned out to be a tough minimization problem. Indeed, the SA scheme prevents the system from remaining trapped in the closest local minimum and has a better chance of finding the global minimum. This is very useful when starting with an initial guess trajectory far from the correct one. To this effect, fictitious masses ($m_f = 0.01$) were assigned to the Fourier coefficients. The resulting equations of motion were integrated using $\delta t = 0.1$ fs and the velocity Verlet algorithm. We started with a fictitious kinetic energy of $T_f = 10^5$ K, and in a few million steps, we reduced it to 10^{-3} K. The average physical kinetic energy of the relaxed trajectory was about 300 K. This trajectory was then used as an input for the minimization of the S_Θ via the conjugate gradient, and at the end of this process, we made the real action ($\mu = 0$ in eq 2) stationary via the conjugate residual method.[11] Despite all this care, the trajectory thus obtained was not perfect. One reason is that the procedure of minimization and local search for the nonpositive definite stationary point is computationally expensive, and one stops at a certain level of the quality factor. One can get a measure of the quality of the path by monitoring the relative difference ΔF between forces and accelerations along it: in a Newtonian trajectory, this is zero. Instead, we found that the distribution of $\Delta F/F$ is broad with a maximum at 0.162. Although in 86% of the cases ΔF had the correct sign, this outcome called for further improvements. Another reason for their difference, and in our opinion, the most important, is the total time of the ADD trajectory (a few ps) compared to that of the true one (nanoseconds). Therefore, we chose to stop the minimization at a certain level, far enough (as we will see below) to obtain the main features of the mechanism, and generate short standard trajectories to recover dynamical aspects.

Dynamical Trajectories. However, despite its limits, the ADD trajectory is quite instructive. Having imposed that the A-to-B transition has to take place in a very short time, it turns out that the reaction coordinate monotonically increases with time. This is an artifact, but it allows us to parametrize the trajectory with respect to q_{ROT}. The total nonbonded energy is shown in Figure 2 as a function of q_{ROT}. The initial oxidized state (A) represents a metastable configuration due to the strong electrostatic repulsion between the charged TTF and CBPQ. After an initial decrease in energy, the system reaches a minimum (Ã) and then, from $q_{ROT} = 0.30$ to $q_{ROT} = 0.40$, climbs over an energy barrier. This prompted us to look for reactive trajectories in the range $q_{ROT} = 0.30-0.45$. Along the ADD path, we chose 66 configurations. Starting from each of the 66 points, we obtained trajectories in the following way. After extracting a set of velocities from a Maxwell−Boltzmann distribution at 300 K, we started a first trajectory followed by a second one with inverted initial velocities for a total of 50 + 50 ps. We repeated this procedure 10 times for each extracted configuration. We used a thermostat set at 300 K in order to avoid an excessive heating of the system. In proximity to a transition state, the two trajectories with the assigned and the inverted velocities may fall into distinct basins of attraction, thus allowing transition states and energy minima to be located. Discrimination between the different basins is made using the variable q_{ROT}, with the condition that the distance between two basin centers be at least 0.06. Of these, 19 connect two different basins. However, when prolonging the trajectory forward and backward in time for a total length of 4 ns, 18 turned out to join local minima while only one was able to connect Ã to the final state B, as it started at $q_{ROT} = 0.45$ and ended in $q_{ROT} = 0.18$ and $q_{ROT} = 0.50$, respectively, passing through different energy minima and transition states (see Figure 3). Thus, this particular reactive trajectory, with the total time increased to 3 + 3 ns, was analyzed in order to obtain an understanding of the overall reaction mechanism. As shown in Figure 3, the time needed for the co-conformational rearrangement from Ã to B (around 600 ps) is much shorter than the overall simulation time but still very long. Obtaining such a long reactive trajectory in a direct way is computationally demanding because of either the presence of several energy minima or the diffusive character of the process. To the best of our knowledge, this is the first time in which such a long dynamical reactive trajectory has been determined. In principle, other approaches[26,27] are meant to address the problem of diffusive reactive behavior but have to make some assumption.

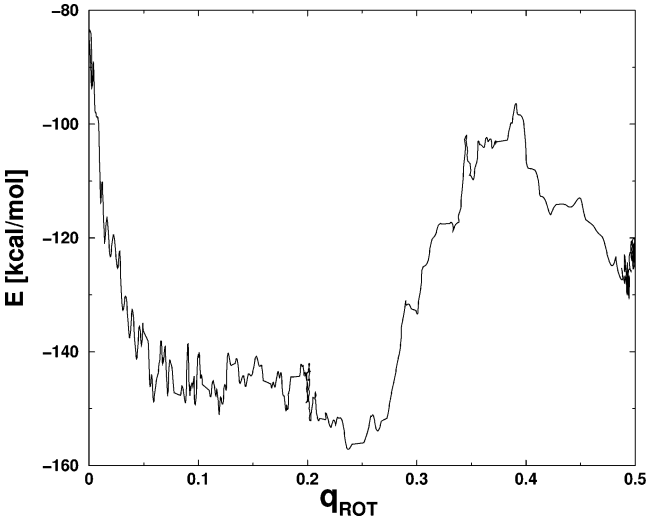

Figure 2. Nonbonded potential energy evaluated along the ADD trajectory.

The CPU time spent minimizing the ADD trajectory and that for the whole procedure to obtain the final dynamical trajectories is almost the same, approximately 2 weeks using a Xeon 2.0 GHz processor.

Analysis of the Microscopic Mechanism. We now analyze the reactive trajectory in Figure 3. This qualitative description is substantiated by the detailed analysis in Figure 4 (colored lines) using the order parameters defined in Section 3. The

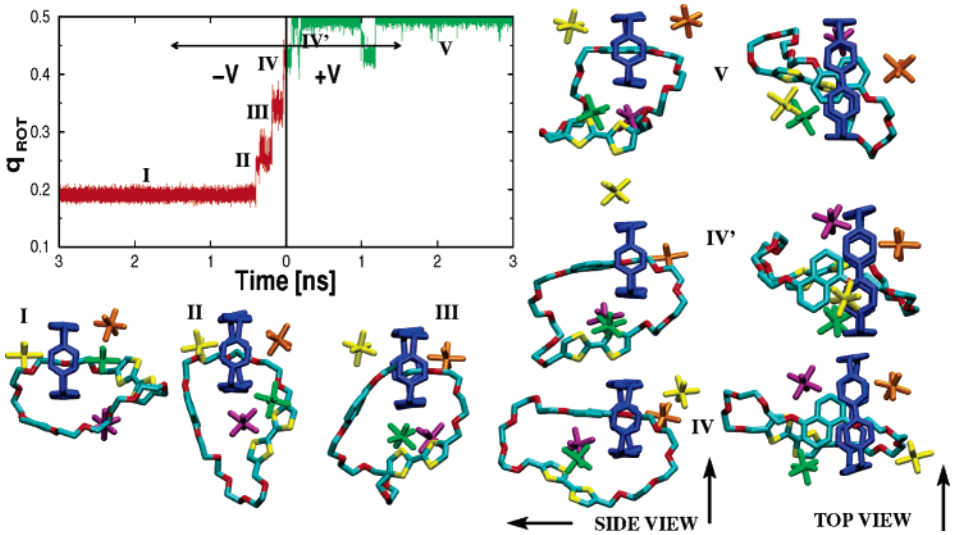

Figure 3. Standard MD trajectory started at the point of the ADD path with $q_{ROT} = 0.45$. Initial conditions for the green trajectory were obtained by inverting the signs of all initial velocities for the red trajectory. Conformers are extracted from different basins of attraction and labeled with Roman numerals.

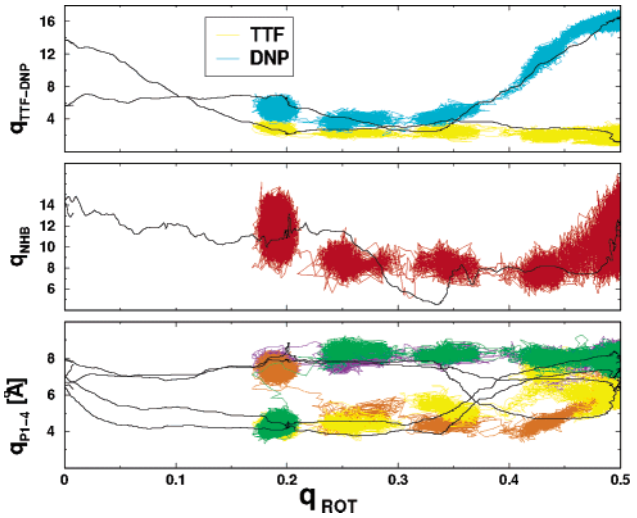

Figure 4. Analysis of the ADD (black lines) and standard (colored lines) trajectories with respect to q_{ROT}. Distances are in Å. The color code used for the counterions is the same as that in Figure 3.

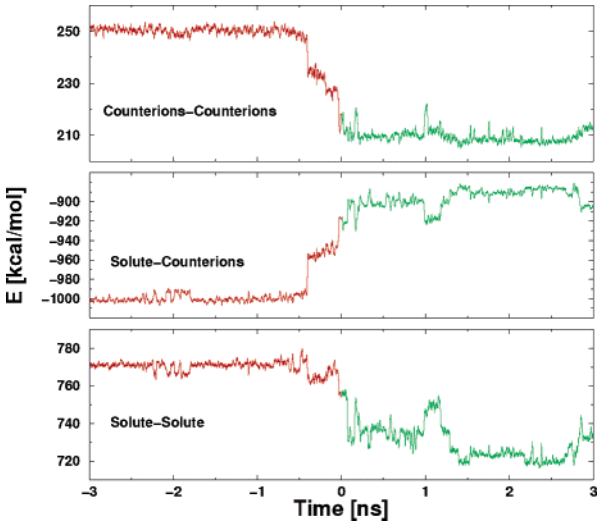

Figure 5. Potential energy terms along the MD trajectory.

analysis of the ADD trajectory (black lines) is also shown for comparison. The evolution of coordinates in ADD shows a contraction relative to the dynamical path, due to the different time scale, but the qualitative features of the trajectory are well-reproduced.

It is seen in Figure 3 that the reaction proceeds through jumps between a succession of local minima. Upon inspection of the main co-conformers, the two halves of the reactive trajectory can be ascribed to different processes, that is, the movement of the DNP unit around the CBPQ cage, from $q_{ROT} = 0.18$ to 0.45, and the attainment of the final state, from $q_{ROT} = 0.45$ to 0.50. Minimum **I** is characterized by a strong $\pi-\pi$ stacking interaction between DNP and CBPQ, with the TTF being expelled just outside the CBPQ ring. In **II** and **III**, the rotation of the crown ether proceeds and the DNP has a T-like orientation relative to CBPQ. The two minima differ from **I** mostly for the different conformation of the crown ether: the different number of hydrogen bonds between the ether ring and CBPQ (q_{NHB} changed from 11 to 8) indicates a lack of electrostatic interactions and larger mobility for the crown ether. In **III**, the DNP assumes a posture already favorable to the insertion into CBPQ. The insertion initiates in **IV** and is accompanied by a coordinated movement of counterions that favors the process. States **IV** and **IV′** differ in the different arrangement of the counterions and in the conformation of the crown ether, which begins to form a set of stabilizing hydrogen bonds. Finally, in **V**, the insertion is complete: the crown ether maximizes the number of hydrogen bonds ($q_{NHB} = 12$) while the counterions are pushed away by stericity.

It should be noted that the green and yellow counterions in Figure 3 from **II** to **IV** accompany the movement of TTF from one side of CBPQ to the other, shielding the electrostatic repulsion. In passing from **III** to **V**, the yellow counterion moves from one side of CBPQ to the other, favoring first the rotation and then the insertion of DNP. This concerted movement of counterions and aromatic units, unusual in solution, is not surprising in light of recent static simulations[1] showing the strong association between counterions and the CBPQ cage in self-assembled monolayers of [2]rotaxanes.

Energy Analysis. From Figure 2, it can be seen that the final state (B) is higher in energy by 20 kcal/mol relative to Ã. To focus on this fact, we decomposed the potential energy in three terms, defined as solute−solute, solute−counterions, and counterions−counterions, see Figure 5. The final result depends largely on an increase of the solute−counterions term, the

Coulomb interactions, because of the fact that the distances between the counterions and CBPQ are longer (see bottom panel of Figure 4). In contrast, the internal solute and counterions' energies decrease, but less than in the previous term, leading to a final metastable state. We expect this effect to become less important in terms of energy, but still present, when considering a more realistic model including an explicit solvent or a solid-state support where counterions have a reduced mobility.

5. Conclusions

Our scheme provided a long reactive trajectory for the co-conformational rearrangement involved in the switching process of a [2]catenane, allowing us to carry out a detailed analysis of its microscopic mechanism. Along the trajectory connecting the reactant and product states, we find several intermediates due to the combination of $\pi-\pi$ and electrostatic interactions. Although previous investigations based on static calculations[24] have already addressed this feature, our approach takes into account dynamical effects. In particular, the key role of counterions within a concerted mechanism is observed: because of the charge of the system, they compete with the TTF and DNP units to stay close to CBPQ. Therefore, we predict a major role of both solvent molecules and ionic species when [2]-catenanes are self-assembled over charged surfaces, where such components may give rise to relevant electrostatic and steric effects.

Finally, this study also provides clear evidence of the ability of the ADD strategy to catch the important features of a dynamical transition between two stable basins in a real system. The multiminimum feature of the process does not allow a complete description using a short (3 ps) ADD trajectory. Rather, the latter serves as a useful starting point for a standard MD approach, allowing the different phases of the circumrotation process to be explored in depth. In particular, the two methods provide very similar mechanisms, with slight discrepancies mainly in the fluctuations allowed by the longer transition time of the trajectory obtained with the standard MD method. The benefit of combining ADD and dynamical trajectories instead of using the alternative TPS scheme is essentially double. The ADD trajectory is already relaxed in the path space, avoiding a long relaxation within the TPS scheme, and it provides a unique trajectory even in the case of a multiminimum mechanism, where the TPS should be applied several times.

Acknowledgment. This work was funded by TopNano21, Project Number 6159.2.

References and Notes

(1) Jang, S. S.; Jang, Y. H.; Kim, Y.; Goddard, W. A., III; Flood, A. H.; Laursen, W. B.; Tseng, H.; Stoddart, J. F.; Jeppesen, J. O.; Choi, J. W.; Steuerman, D. W.; Delonno, E.; Heath, J. R. *J. Am. Chem. Soc.* **2005**, *127*, 1563−1575.

(2) Collier, C. P.; Mattersteig, G.; Wong, E. W.; Luo, Y.; Beverly, K.; Sampaio, J.; Raymo, F. M.; Stoddart, J. F.; Heath, J. R. *Science* **2000**, *289*, 1172−1175.

(3) Balzani, V.; Venturi, M.; Credi, A. *Molecular Devices and Machines*; Wiley-VCH: Weinheim, Germany, 2003.

(4) Pease, A. R.; Jeppesen, J. O.; Stoddart, J. F.; Collier, C. P.; Heath, J. R. *Acc. Chem. Res.* **2001**, *34*, 433−444.

(5) Balzani, V.; Credi, A.; Raymo, F. M.; Stoddart, J. J. *Angew. Chem., Int. Ed.* **2000**, *39*, 3348−3391.

(6) Torrie, G. M.; Valleau, J. P. *Chem. Phys. Lett.* **1974**, *28*, 578−581.

(7) Laio, A.; Parrinello, M. *Proc. Natl. Acad. Sci. U.S.A.* **2002**, *20*, 12562−12566.

(8) Bolhuis, P. G.; Dellago, C.; Chandler, D. *Faraday Discuss.* **1998**, *110*, 421.

(9) Dellago, C.; Bolhuis, P. G.; Csajka, F. S.; Chandler, D. *J. Chem. Phys.* **1998**, *108*, 1964−1977.

(10) Passerone, D.; Parrinello, M. *Phys. Rev. Lett.* **2001**, *87*, 108302.

(11) Passerone, D.; Ceccarelli, M.; Parrinello, M. *J. Chem. Phys.* **2003**, *118*, 2025−2032.

(12) Anelli, P. L.; Ashton, P. R.; Ballardini, R.; Balzani, V.; Delgado, V. B. M.; Gandolfi, M. T.; Goodnow, T. T.; Kaifer, A. E.; Philip, D.; Pietraszkiewicz, M.; Prodi, L.; Reddington, M. V.; Slawin, A. M. Z.; Spencer, N.; Stoddart, J. F.; Vicent, C.; Williams, D. J. *J. Am. Chem. Soc.* **1992**, *114*, 193−218.

(13) Badjic, J. D.; Balzani, V.; Credi, A.; Silvi, S.; Stoddart, J. F. *Science* **2004**, *303*, 1845−1849.

(14) Hernandez, J. V.; Kay, E. R.; Leigh, D. A. *Science* **2004**, *306*, 1532−1537.

(15) Ceccarelli, M.; Danelon, C.; Laio, A.; Parrinello, M. *Biophys. J.* **2004**, *87*, 58−64.

(16) Aktah, D.; Passerone, D.; Parrinello, M. *J. Phys. Chem A* **2004**, *108*, 848−854.

(17) Balzani, V.; Credi, A.; Mattersteig, G.; Matthews, O. A.; Raymo, F. M.; Stoddart, J. F.; Venturi, M.; White, A. J. P.; Williams, D. J. *J. Org. Chem.* **2000**, *65*, 1924−1936.

(18) Brown, C. L.; Jonas, U.; Preece, J. A.; Ringsdorf, H.; Seitz, M.; Stoddart, J. F. *Langmuir* **2000**, *16*, 1924−1930.

(19) Cornell, W. D.; Cieplak, P.; Bavly, C. I.; Gould, I. R.; Merz, K. M., Jr.; Ferguson, D. M.; Spellmeyer, D. C.; Fox, T.; Caldwell, J. W.; Kollmann, P. *J. Am. Chem. Soc.* **1995**, *117*, 5179−5197.

(20) Procacci, P.; Paci, E.; Darden, T.; Marchi, M. *J. Comput. Chem.* **1997**, *18*, 1848−1862.

(21) Grabuleda, X.; Ivanov, P.; Jaime, C. *J. Phys. Chem B* **2003**, *107*, 7582−7588.

(22) Asakawa, M.; Ashton, P. R.; Balzani, V.; Credi, A.; Hamers, C.; Mattersteig, G.; Montalti, M.; Shipway, A. N.; Spencer, N.; Stoddar, J. F.; Tolley, M. S.; Venturi, M.; White, A. J. P.; Williams, D. J. *Angew. Chem., Int. Ed* **1998**, *37*, 333−337.

(23) Parrinello, M.; Rahman, A. *J. Appl. Phys.* **1981**, *52*, 7182.

(24) Deleuze, M. S.; Leigh, D. A.; Zerbetto, F. *J. Am. Chem. Soc.* **1999**, *121*, 2364−2379.

(25) *CPMD*, version 3.5; IBM Corp.: 1990−2001; MPI für Festkörperforschung Stuttgart: 1997−2001.

(26) Moroni, D.; Bolhuis, P. G.; van Erp, T. S. *J. Chem. Phys.* **2004**, *120*, 4055−4065.

(27) Cardenas, A. E.; Elber, R. *Biophys. J.* **2003**, *85*, 2919−2939.